An AOI Approach for IC Lead Index Auto-verification

Der-Baau Perng* Guei-Ci Chang [#], Shu-Ming Lee [+], and Ssu-Han Chen[+]

*: Professor; [#]: Graduate student; [+]: Ph. D.

Department of Industrial Engineering and Management,

National Chiao Tung University, HsinChu, Taiwan 30010

Phone: +886-3-5731866

FAX: +886-3-5722392

E-mail: perng@cc.nctu.edu.tw

Abstract

To wire-bond automatically, the IC lead positions on the CAD drawing and the corresponding ones on the extracted substrate image should be pre-verified. This paper proposed an AOI approach for IC lead index auto-verification which conquered the lead shape distortion, golden exposed, shifting, rotation, and scaling difficulties of extracted substrate image. Experimentations revealed that the proposed AOI approach can accurately verify the corresponding leads between a CAD drawing and the extracted substrate image with high repeatability.

Keywords: substrate, lead verification, particle swarm optimization

1 Introduction

Substrate is a kind of base material that is devised as the intermediary between the integrated circuit (IC) chip and the printed circuit board (PCB). Hundreds of leads spread on the substrate according to the required spec of customers for wire bonding. Traditionally, it is required to confirm the index of each lead on the CAD drawing (Figure 1(a)) corresponding to the extracted substrate image (Figure 1(b)) before the automatic wire bonding process. However, due to a manufactured part can differ from the intended CAD design but be functionally acceptable in practice [Nobel, 1995];

Sixth International Symposium on Precision Engineering Measurements and Instrumentation, edited by Jiubin Tan, Xianfang Wen, Proc. of SPIE Vol. 7544, 754470 · © 2010 SPIE · CCC code: 0277-786X/10/$18 · doi: 10.1117/12.886015

the extracted image, indeed, embeds with variants such as lead shape distortion and golden exposed which is caused by etching or plating process. Furthermore, due to the resolution of CCD and the shifting, rotation, and scaling error of image caused by machine vision system, no any available method can auto-verify the corresponding of lead index. In practice, most IC packaging foundries rely on humans with the aid of microscopes to assign the leads indices between CAD drawing and extracted image. In this way, the indexing can be accurate after repeated examinations. Therefore, manual indexing would be replaced by automated methods to reduce fatigue, save manpower, and improve the automaticity or productivity of wire bonding process.

This paper proposed an IC lead index auto-verification algorithm for distinct pair of the CAD drawing and extracted image of substrate objects. Firstly, a series of image pre-processing methods were devised for lead extraction. The CAD drawing was treated as the template. Then the particle swarm optimization (PSO) method was used for searching a parameter vector of affine transformation that can manipulate the extracted image and yield an affined image to have highest intersection lead area with respective to the template. Accordingly, the intersection lead area of affined image and template formed an overlapping image. Finally, the corresponding lead indices of CAD drawing and the image of substrate can be verified in terms of the overlapping image.

The rest of this paper is organized as follows. In section 2, we described the hardware structure and the software algorithm of the proposed IC lead index auto-verification system. Furthermore, we described the experimental environment and presented the experimentation results. Our concluding remarks and further suggestions were discussed in section 3.

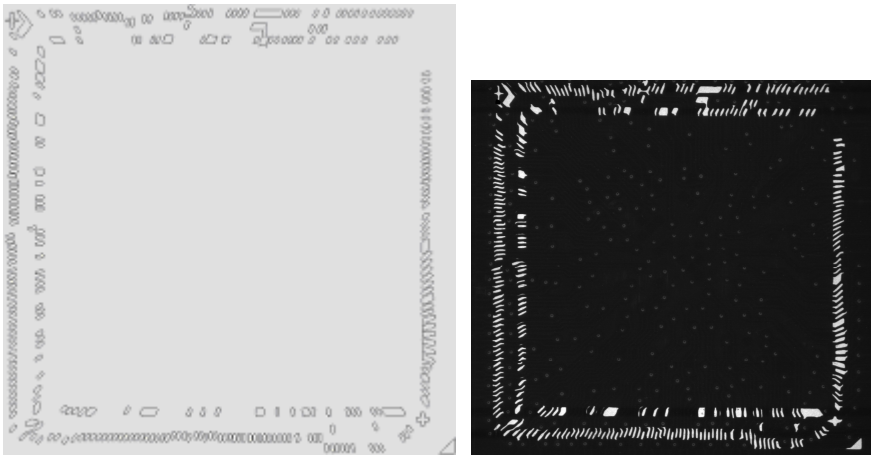

(a) (b)

Figure 1: (a) The designed CAD drawing of a substrate, (b) the extracted image of a substrate

2 Research Methodologies

2.1. Computer vision system

Figure 2 shows the structure of proposed AOI system for IC lead index auto-verification. An image of mounted substrate was captured by a JAI CV-A1 black and white camera with a resolution of 1380×1035, an OPTEM Zoom 125C lens and a Matrox Meteor II frame grabber. The ring LED light was included to supply a uniform and stable front illumination. The apparatus was connected to a computer.

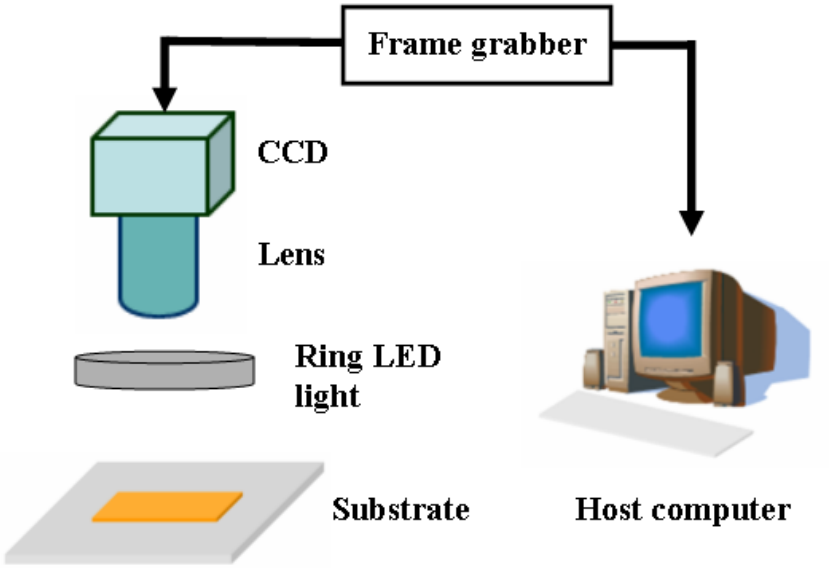

Figure 2: The proposed AOI system for IC lead index auto-verification

2.2. The IC lead index auto-verification algorithm

2.2.1. Lead extraction

To reveal the lead areas in both CAD drawing (Figure 1(a)) and extracted image (Figure 1(b)), a lead extraction function was introduced. Practically, the leads are represented by black contours in the CAD drawing, but are represented by white areas (maybe accompany with some noises) in the extracted image. Because the intrinsic representation of leads in CAD drawing and extracted image is quite different, it should be disposed firstly to have a unique representation. Hence, we used black to represent the front-ground pixel of a lead in the subsequent contents.

For the CAD drawing, the pixel with gray-level that was smaller than the corresponding Otsu's threshold was darkened; otherwise, was whitened. The polygon estimation method was adopted to mend the disconnected or interrupted lead contours. This ensured each lead contour to form a closed region and can then be filled to the full. The minimal bounding rectangular which included all the darkened and filled leads was finally segmented as shown in Figure 3(a), named "Image_CAD".

For the extracted image, the pixel with gray-level that was larger than the corresponding Otsu's threshold was darkened; otherwise, was whitened. Distinct from the faultless CAD drawing, the problem of gold exposed may occur in the real-world process which results in some pseudo leads and appears in the extracted image. We recorded the area feature of each lead and calculated the corresponding statistics, the first and third quartiles (Q_1 and Q_3). The leads whose area were smaller than $Q_1–1.5\times(Q_3–Q_1)$ were regarded as outliers, *i.e.* noises, and were filtrated. After this operation, those pseudo leads were eliminated as far as possible. Finally, the minimal bounding rectangular which included all the darkened leads was segmented as shown in Figure 3(b), named "Image_GET".

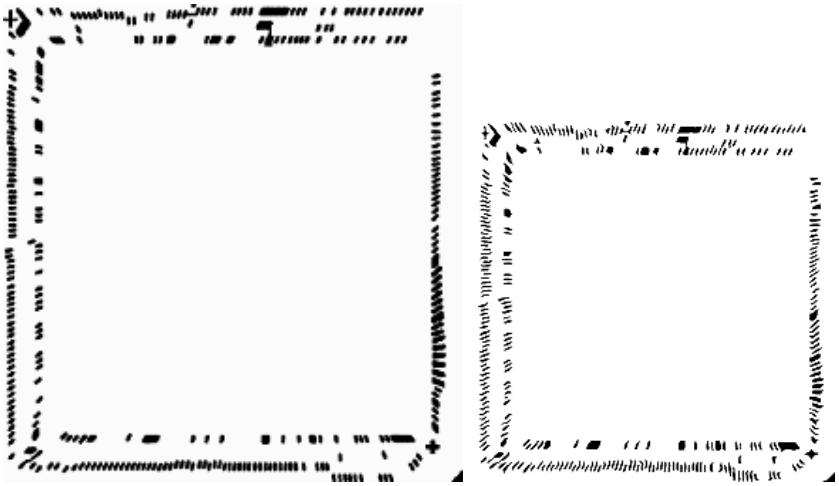

(a) (b)

Figure 3: (a) Image_CAD, (b) Image_GET

2.2.2. Automatic affine transformation by PSO

The real substrates were produced following the spec of the CAD drawing. Even if the shape conditions of distortion and gold exposed phenomena were invertible, some proportional relationship between Image_CAD and Image_GET still existed. To verify the lead labels between Figure 3(a) and Figure 3(b) under an imperfect environment, the Image_GET was first adjusted to be Image_AFF by

using the affine transformation as shown in Equation (1) to have almost the same size and orientation as Image_CAD. That is, given a combination parameter in Equation (1), the Image_GET will be transformed into affine transformation space.

$$\begin{bmatrix} \mathbf{x}'' \\ \mathbf{y}'' \end{bmatrix} = \begin{bmatrix} a_{11}\cos\theta & -\sin\theta \\ \sin\theta & a_{22}\cos\theta \end{bmatrix} \begin{bmatrix} \mathbf{x}' \\ \mathbf{y}' \end{bmatrix} + \begin{bmatrix} b_1 \\ b_2 \end{bmatrix} \tag{1}$$

where $(\mathbf{x}', \mathbf{y}')$ is the pixel intensity in an input image, while $(\mathbf{x}'', \mathbf{y}'')$ is that in output image. a_{11} and a_{22}, respectively, is the scaling factor of x- and y-axis, θ is the rotation degree, and b_1 and b_2, respectively, is the shift distance in x- and y-axis. A proper resultant Image_AFF was given in Figure 4(a). The fitness evaluation function was given in Equation (2),

$$\text{Maximum} \sum_{n=1}^{N}\sum_{m=1}^{M}\left[\text{Image\_CAD}(m,n) \text{ NOR Image\_AFF}(m,n)\right] \Big/ MN \tag{2}$$

where $M \times N$ is the size of the overlapping image, NOR is the digital logic NOR gate. An output 1 results if the gray-levels of both Image_CAD and Image_AFF to the gate are 0. If any one inputs is 1, an output 0 will be resulted. The higher the fitness value was, the more overlapping area of the leads between Image_CAD and Image_AFF would be. That is, when Image_AFF was superimposed over Image_CAD, as shown in Figure 4(b), the corresponding fitness value was estimated by Equation (2). The overlapping area was marked in black as shown in Figure 4(c), named “Image_OLP”.

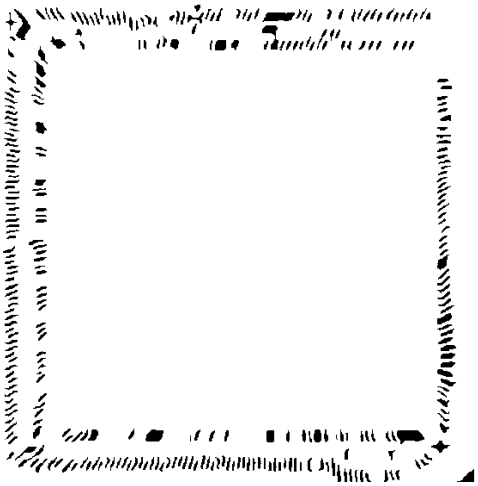

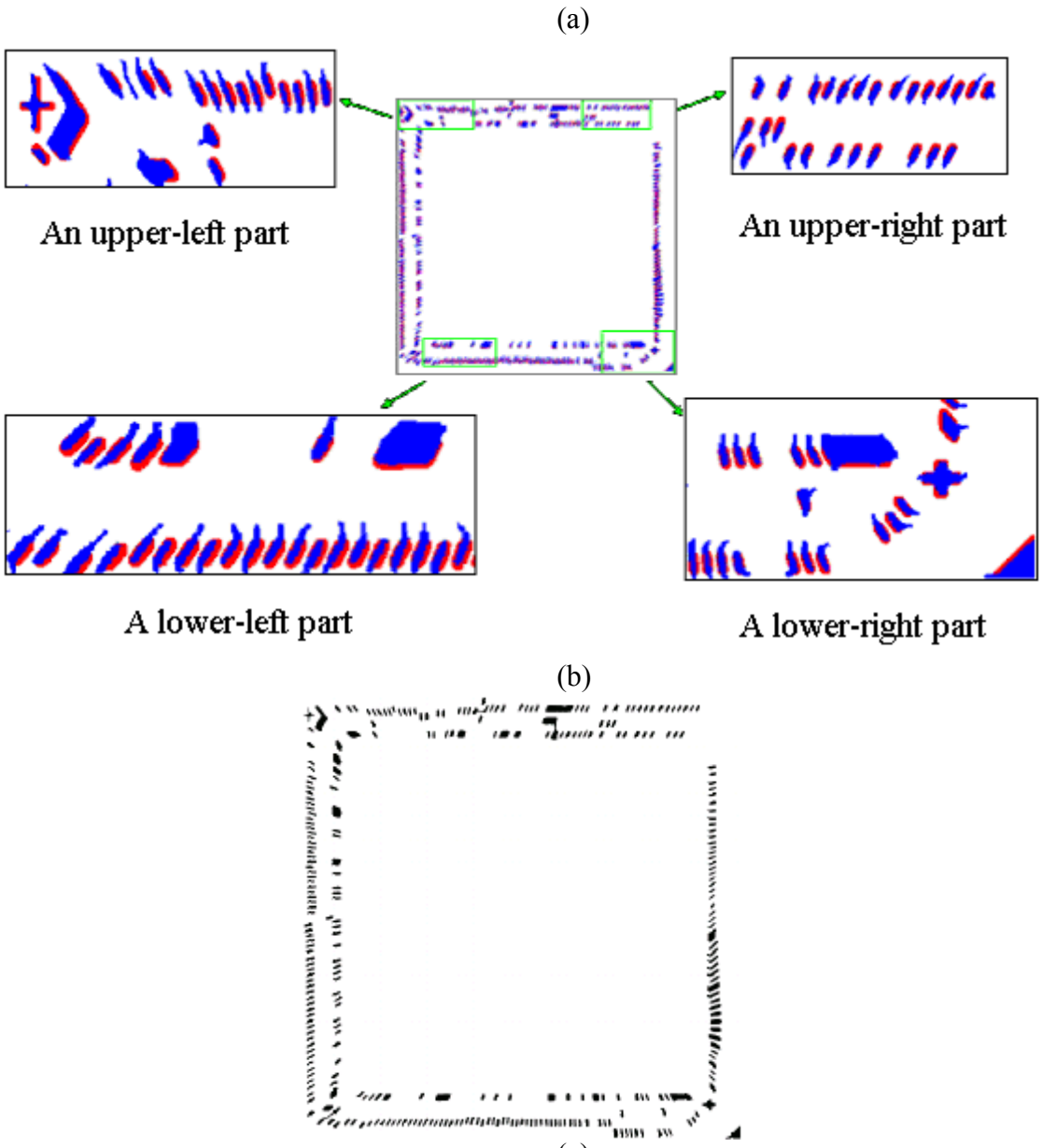

Figure 4: (a) Image_AFF, (b) superimposed Image_AFF (blue) over Image_CAD (red), (c) resultant Image_OLP

To reduce the search space of the affine transformation and not to try exhaustively, we adopted an automatic stochastic search algorithm, PSO. Each particle in PSO was formulated as a vector of size 1×5 pixels with respective to a_{11}, a_{22}, θ, b_1, and b_2 in Equation (1). Let there be P particles, each with associated positions $\mathbf{x}_i$ and velocities $\mathbf{v}_i$, i = 1, 2, …, P. In this paper, P was set to 20 and the

corresponding sensitivity analysis can be found in [Chang, 2009]. Let $\mathbf{p}_i$ be the current best position (with best fitness) of each particle and let $\mathbf{g}$ be the global best. After initializing $\mathbf{x}_i$ and $\mathbf{v}_i$ for all i, they can be updated by,

$$\mathbf{v}_i(t+1) = w \times \mathbf{v}_i(t) + c_1 \times \mathbf{r}_1 \times [\mathbf{p}_i(t) - \mathbf{x}_i(t)] + c_2 \times \mathbf{r}_2 \times [\mathbf{g}(t) - \mathbf{x}_i(t)] \quad (3)$$

$$\mathbf{x}_i(t+1) = \mathbf{x}_i(t) + \mathbf{v}_i(t+1) \quad (4)$$

where t = 1, 2, …, T denotes the generation step. T denotes the number of maximum generation, $\mathbf{r}_1$ and $\mathbf{r}_2$ are random value vectors in the range of [0, 1]. The inertia weight factor, w, provides the necessary diversity to the swarm by changing the particles at the local optima. In the paper, the inertia weight would be reduced linearly from 0.8 to 0.4 at each generation to ensure good convergence. The cognitive and social learning rates, c_1 and c_2, respectively, controls how much the particle's personal best and global best will influence the movement. Here, both c_1 and c_2 are set as 2. Then the local and global best fitness values are updated at each generation, based on Equations (5) and (6),

$$\mathbf{p}_i(t+1) = \mathbf{x}_i(t+1), \text{ if } f[\mathbf{x}_i(t+1)] > f[\mathbf{p}_i(t)] \quad (5)$$

$$\mathbf{g}(t+1) = \mathbf{x}_i(t+1), \text{ if } f[\mathbf{x}_i(t+1)] > f[\mathbf{g}(t)] \quad (6)$$

where the symbol f denotes the fitness evaluation function. Not until the limit of generations was achieved, the iteration loop kept working. In this paper, the number of maximum generation T was set to 100 and the corresponding sensitivity analysis can be found in [Chang, 2009]. As shown in Figures 5 and 6, when the generation increases, there exists more and more overlap as well as higher and higher fitness value. The final result, as shown in Figure 5(c), whose fitness value was equal to 0.0331, the corresponding global best particle was 1.276, 1.286, 0.210, -2.756, and 1.340 with respective to a_{11}, a_{22}, θ, b_1, and b_2.

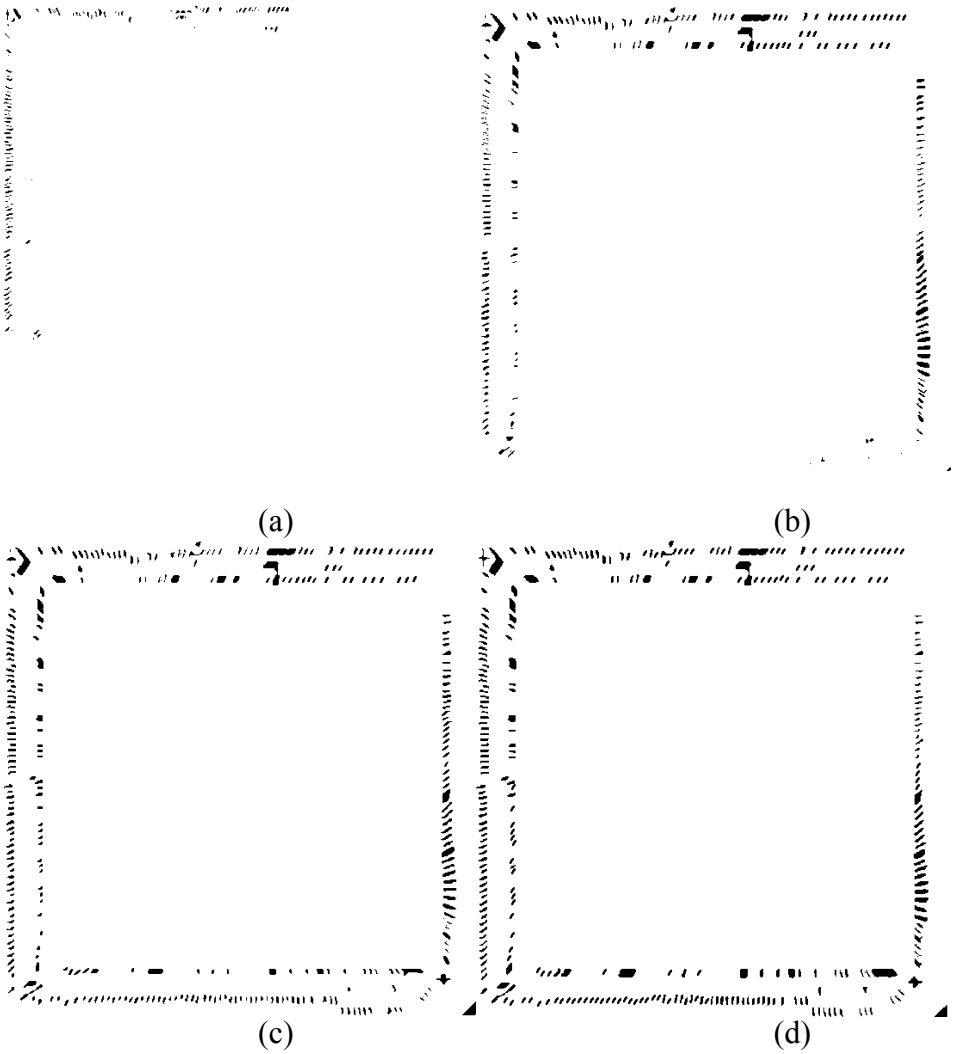

Figure 5: the Image_OLP when (a) t = 1 (fitness = 0.0036), (b) t = 10 (fitness = 0.0169), (c) t = 40 (fitness = 0.0254), (d) t = 60 (fitness = 0.0319)

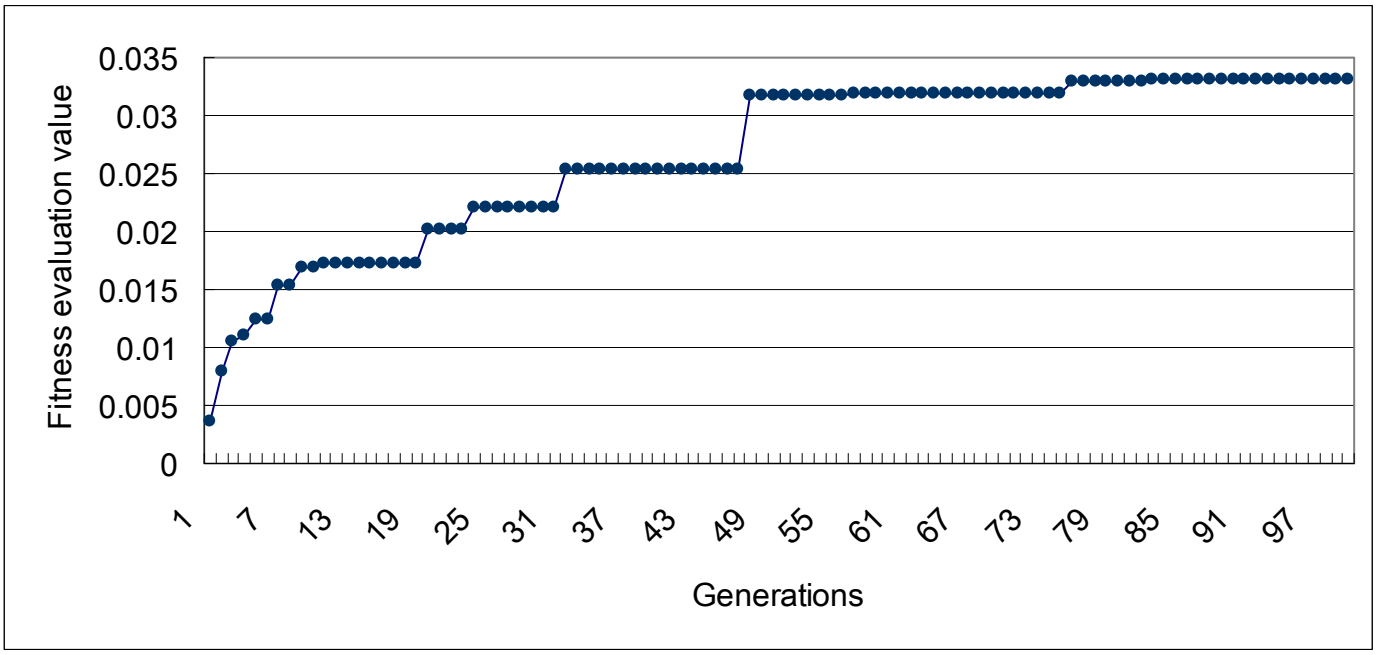

Figure 6: number of generations vs. fitness evaluation values

2.2.3. Lead index verification

To verify the lead index, we first recorded the top-left coordinate of each overlapping area in Image_OLP as shown in Figure 7(a). Then the connected component labeling (CCL) algorithm was implied to Figure 7(a). As a consequence, each isolated blob in Figure 7(a) would have a unique index and formed a labeled image, named "Image_SEED" (described later). The labeled image could then be superimposed back over the Image_CAD and Image_AFF separately as shown in Figures 7(b) and 7(c). Due to the upper-left coordinate of each overlapping area in Figure 4(c) is a pixel element of the corresponding intersection area, it is to locate the region of each lead on both Image_CAD and Image_AFF when back superposition was executed. We treated each isolated blob as a seed, spread it on Image_CAD and Image_AFF separately, and implied seeded region growing algorithm to grow the corresponding inferential region and replace the gray-level following the corresponding index of the seed. The element of background and remained blobs that has no corresponding seed (as shown in Figure 7(d)) would be assigned a gray-level of zero. In this way, the lead indices between

Image_CAD and Image_AFF were verified successfully. The enlarged labeled output pair was demonstrated in Figure 8. Finally, the original coordinates of extracted image can be restored by transforming the Image_AFF using inverse affine transformation.

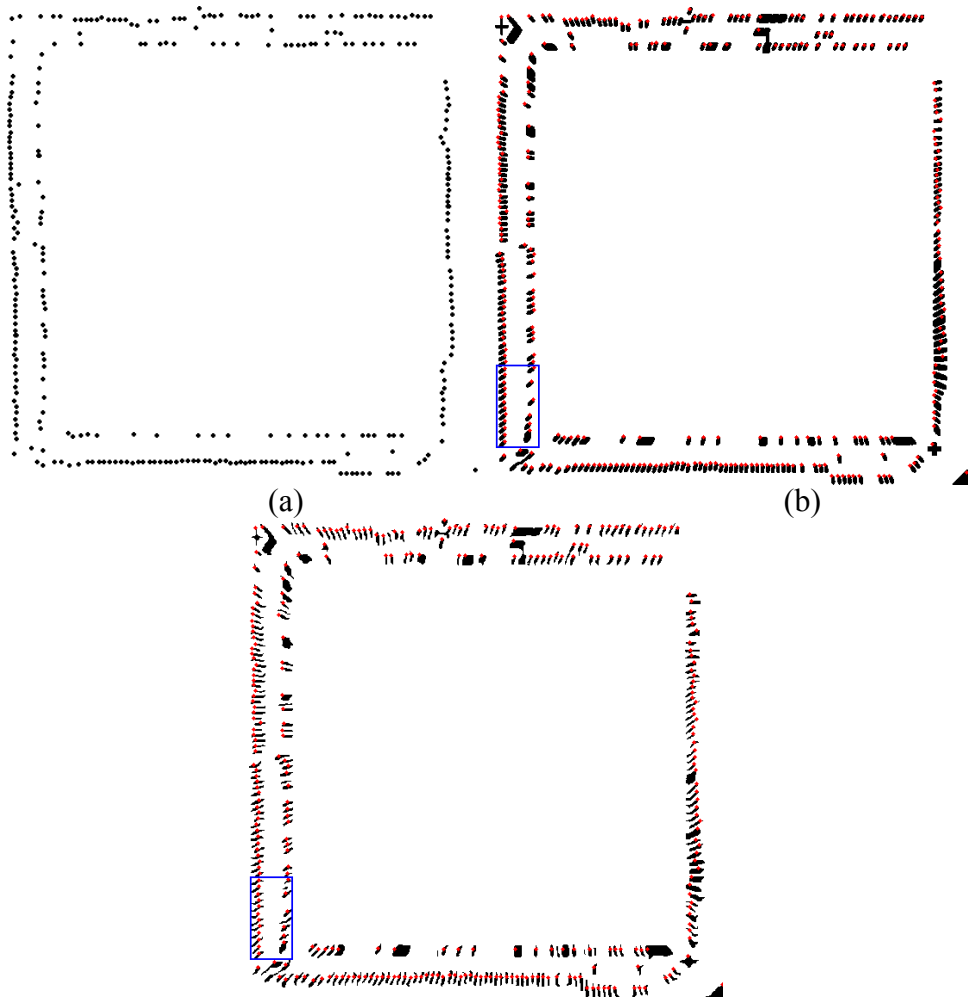

(a) (b)

(c)

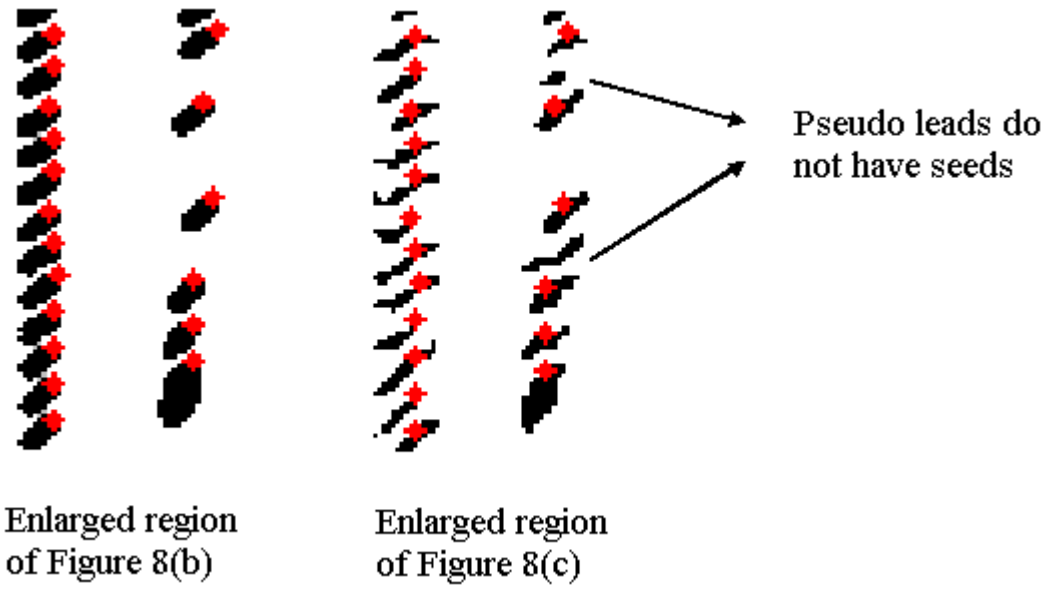

(d)

Figure 7: (a) Image_SEED, (b) the seeds mapped onto Image_CAD, (c) the seeds mapped onto Image_AFF, (d) the enlarged regions of the blue rectangular of Image_CAD and Image AFF

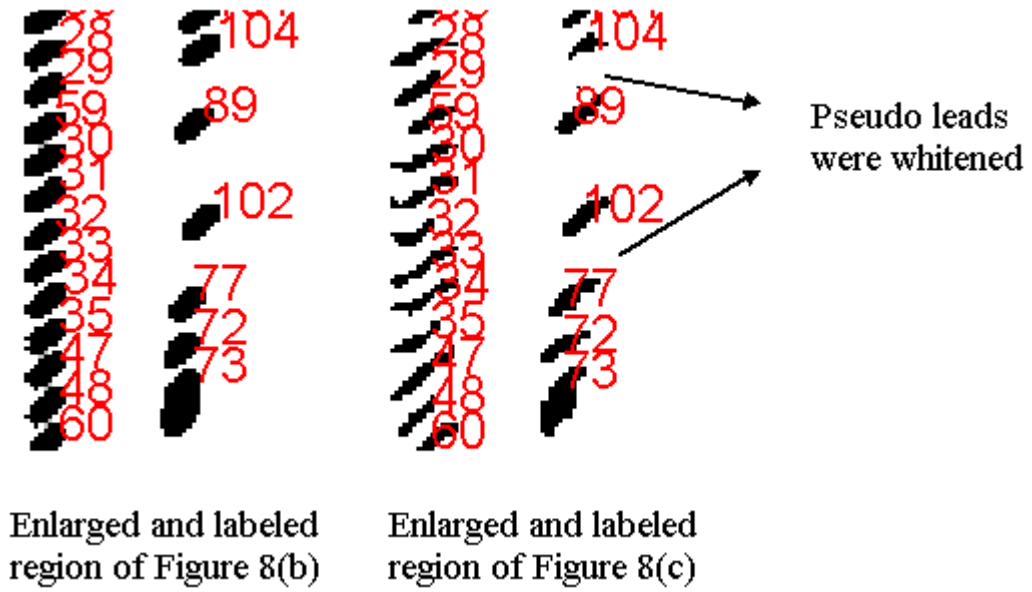

Figure 8: Resultant labeled Image_CAD and Image_AFF

3 Conclusions and suggestions

With the increasing complexity of substrates, manual lead index verification of CAD drawing

and corresponding extracted image in IC packaging industry still cannot beat the lead varieties robustly. An IC lead index auto-verification algorithm is highly required. In this paper, an AOI system for IC lead index auto-verification was proposed and implemented. The proposed method revealed high repeatability and wide generalization ability. However, the proposed method took about 725 seconds in verifying the lead indices of Figure 1 when the number of iterations and particles, respectively, was set equal to 100 and 20. Even if the time cost has considerably outperformed than that of manual verification, it is worth studying how to reduce the auto-processing time for further research.

Acknowledgements

This research is partially supported by the National Science Council, Taiwan, under contract No. NSC 96-2221-E-009-077-MY3.

References

[1] Chang G. C., *An AOI approach for IC lead verification,* Master thesis, Department of Industrial Engineering and Management, National Chiao Tung University, Hsinchu, Taiwan, 2009.

[2] Eberhart R. C. and Kennedy J., "A new optimizer using particle swarm theory," *Proceedings of the 6th International Symposium on Micromachine and Human Science*, pp.39-43, 1995.

[3] Kennedy J., "The particle swarm: social adaptation of knowledge," *IEEE International Conference on Evolutionary Computation*, pp.303-308, 1997.

[4] Noble J. A., "From inspection to process understanding and monitoring: a view on computer vision in manufacturing," *Image and Vision Computing*, 13(3), pp.197-214, 1995.

[5] Shi Y. and Eberhart R. C., "Parameter selection in particle swarm optimization," *Proceeding of 7th Annual Conference on Evolutionary Programming*, pp.591-601, 1998.